

## Analysis of the Triggering Mechanism of the Square Thin-Walled Absorber

Michał Rogala<sup>1\*</sup>, Jakub Gajewski<sup>1</sup>

<sup>1</sup> Faculty of Mechanical Engineering, Department of Machine Design and Mechatronics, Lublin University of Technology, ul. Nadbystrzycka 38, 20-618 Lublin, Poland

\* Corresponding author's e-mail: m.rogala@pollub.pl

### ABSTRACT

The aim of the research is the analysis of thin-walled aluminum profiles with embossed crush initiator. Samples with square cross-section loaded dynamically were studied until the complete loss of velocity by the tup. The numerical analyses were based on an elastic-plastic material model. The material properties of AA-6063 aluminum were derived from own tests performed on a tensile machine. The analyses were conducted using the numerical method (Abaqus CAE). Using a dynamic testing machine, the obtained numerical data were verified on the basis of models showing the best improvement in crush efficiency indicators. In the experimental study, high-speed camera images were used to identify the forming plastic hinges. Based on the obtained results of experimental and numerical analysis, crush efficiency indicators were determined and compared. It was determined that the use of a passive energy absorber increases the efficiency of the crushing force by around 50%, in addition, the correct location of the crush initiator allows to gain 15%. The results of the study showed that proper placement of the crush initiator decrease Peak Crushing Force (PCF) while increasing mean crushing force (MCF).

**Keywords:** thin-walled structures, crashworthiness, finite element method, passive absorber.

### INTRODUCTION

Today, passive safety is a particularly important design aspect of mechanical structures. Vehicles have specific crumple zones designed to protect vehicle components during a road crash. Particularly important is the crash-box, which protects the passengers in a frontal collision at a maximum speed of 15–20 km/h without damage to the vehicle stringers. A passive energy absorber is characterized by the fact that, with certain design assumptions, the structure folds like an accordion to absorb mechanical energy without generating large overloads. The field of energy absorption by vehicle protective components began in the early 1960s. Before that, vehicles had rigid steel bumpers to protect the occupants, but because of the overloads generated during an accident, they could be fatal to the passengers. The first scientific paper in this area came from 1960s

when Alexander [1] determined the behavior of thin-walled circular columns subjected to axial crushing. In the following years, research on the failure behavior of columns was addressed, and mathematical models were described for both circular and square sections [2–4]. As the passive safety has developed, monographs have appeared that describe in depth the behavior of thin-walled structures in post-buckling dynamic crush. They have also described the effects of overloads and pulse duration on the damage that can occur during a collision [5,6]. To enhance the absorber, researchers have begun disturbing the geometry to change its behavior and improve crush efficiency indicators. The geometric perturbation, called a crush initiator or trigger, can initiate a crush at a precise location [7]. This involves the form of buckling of the column and the number of half-waves that can be produced during dynamic crushing, which significantly affects the energy

efficiency of crash boxes [8]. Initially the crush initiators took the shape of transverse bends on the side wall, with time they started to take more complicated shapes, both in the form of holes or bends, which dramatically change the behavior of thin-walled profile, especially at the beginning of process during forming of the first fold [7,9]. Due to nature of the energy absorber, the crush mechanism is based on the plastic deformation of thin-walled metal columns at the expense of absorbed mechanical energy. Passive structures have various crush initiators; a common approach is to make notches across the profile. Such initiators were used by Kaczynski et al. [10] for pyramids made of magnesium. In their study, they demonstrated the impact of notch placement on ability of structure capacity of thin-walled contraptions. Another method of crush initiation was presented by Ferdynus et al. [11] by making embossments on the edges of a column with a square cross section. Spherical embossments of different diameters and depths were made in aluminum columns. Experimental studies showed a significant effect of the embossing depth on the peak of the crush initiation force, as well as the total efficiency of the passive energy absorber. A different way to initiate the crush process is to make cutouts in the column, which reduce forces value in the direction of crushing [12,13]. The tubular energy absorber with holes showed stable crush and the occurrence of annular form. A novel approach for initiating the crush process of a passive energy absorber was presented by Peixinho et al. [14] using thermally annealed zones. This approach does not cause discontinuities in the material that can result in wall rupture. The thermally made crush initiator results in plasticization of the material and a decrease reaction force detected at the initiate stage. Despite the positive implications, improper zone heating on the column can result in non-axial crush and even global buckling.

Due to limited space, crash-boxes must have a certain length, which is related to the ability of thin-walled sections to absorb energy. In order to increase their efficiency, researchers have proposed using fillings inside which can absorb additional mechanical energy. The first performance enhancements encountered were multi-cell structures [15], which had additional walls inside in 3x3 or 4x4 arrangements that absorbed additional energy while maintaining the same external column dimensions. With the development of technology, researchers have used metal porous

structures that exhibit good energy-absorption properties as filler [16–19]. In particular, aluminum foams with both open and closed pores are often used. Due to the frequent use of multivariate analysis, it is common to applied neural networks in data analysis [20–23]. Optimization of many parameters is time consuming, and the use of ANN (artificial neural network) allows to reduce the time of analysis while maintaining high reliability of the obtained results. Currently in the world literature, a common approach in the study of passive safety is the use of fiber composites [24–28], however, due to the high susceptibility of the structures to microdamage their use in industry has still not come to fruition, and their application is unitary in selected engineering structures. In order to shorten the analysis finite element method is used [29–31], which allows to achieve high quality data with relatively low computational cost.

The research presented here undertakes different locations of the crush initiator, which, according to the authors, can change the form of buckling and, consequently, the formation of plastic hinges. The location of the crush initiator can then change the energy-absorbing capacity of the crush initiator. The importance of the topic undertaken is due to the widespread use of closed-section profiles in engineering as structural elements. The initiation of deformation has a significant impact on the course of failure of a thin-walled structure. Correct modeling of thin-walled columns can allow the use of the column as a load-bearing element while using it as a passive energy absorber. To determine the performance of thin-walled structures, crush efficiency indices are commonly encountered in the literature. All the crush characteristic quantities can be determined from the force-shortening diagram (Figure 1). The first characteristic quantity is the mechanical energy dissipate, specified as the area below the function line i.e. the integral of the function over displacement derived by the following Equation 1:

$$EA(dx) = \int_0^{dx} F(x)dx \quad (1)$$

Further values presented above is Peak Crushing Force (PCF) indicator, for typical absorber a peak value noticeable at the beginning of crush, while Mean Crushing Force (MCF) index is the average value obtained during the whole crush presented as follows:

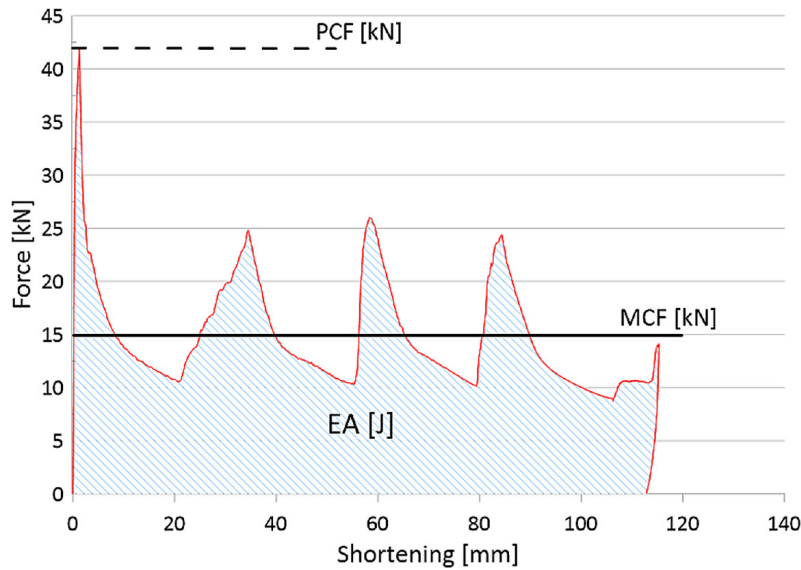


Figure 1. Example force curve in a function of shortening

$$MCF = \frac{EA(dx)}{dx} \quad (2)$$

On the basis of above mentioned indicator, the first coefficient can be calculated Crush Load Efficiency (CLE), and it present relation of the average and peak force value using the formula below:

$$CLE = \left( \frac{MCF}{PCF} \right) 100\% \quad (3)$$

where: *PCF* – peak crushing force; *MCF* – mean crushing force.

The last index is the Stroke Efficiency (SE), defined as dependence of crushing distance to weight of the column, and is presented by formula 4:

$$SE = \frac{L_o - U}{L_o}, [-] \quad (4)$$

where: *U* – shortening of column; *L<sub>o</sub>* – Initial length of a column.

### ANALYTICAL EQUATION

In analyzing thin-walled dynamically crushed profiles, we can derive analytical relationships based on geometric parameters. Based on the geometric parameters shown in Figure 2, the following equations can be deduced. The relationships shown below are derived from extensive research work presented by Jones [5]. Taking into account during deformation the fold is shaped in a symmetrical manner, all the mathematical formulas mentioned below are applicable in analyzed case. The first

magnitude is energy consumed through collapsing thin-walled element, defined by Equation 5:

$$E = M_0 \left( 16HI_1 \frac{b_f}{t} + 2\pi c + 4I_3 \frac{H^2}{b_f} \right) \quad (5)$$

where: *I<sub>1</sub>*, *I<sub>3</sub>* – integrals; *c* – two widths of the profile

Analyzing the performance of the crushing distances, we can conclude that there is a symmetrical mode of collapse,

$$\frac{\delta_c}{2H} = 0.77 \quad (6)$$

where:  $\delta_c$  – crushing distance; *2H* – height of plastic hinge.

To specify an MCF value, it is necessary to define the relation defining the coefficient of plastic strain. To do this, the Cowper-Symonds model was applied:

$$\frac{\sigma_d}{\sigma_s} = 1 + \left( \frac{\dot{\epsilon}}{C} \right)^{\frac{1}{P}} \quad (7)$$

where:  $\sigma_d$  – dynamic yield stress;  $\sigma_s$  – static yield stress;  $\dot{\epsilon}$  – strain rate.

Taking into account the above equations, the analytical MCF in dynamic crush is defined below.

$$\frac{F_m^d}{M_0} = 52.22 \left( 1 + \left( 0.33 \left( \frac{V}{cC} \right)^{\frac{1}{P}} \right) \left( \frac{c}{t} \right)^{\frac{1}{3}} \right) \quad (8)$$

where:

$$M_0 = \sigma_0 \frac{t^2}{4}$$

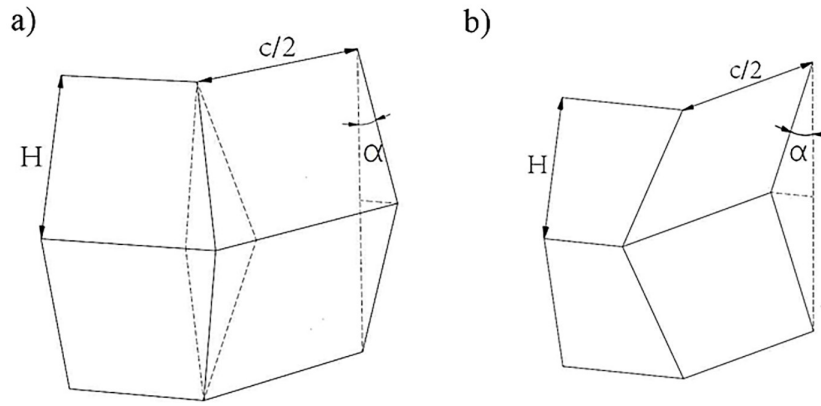


**Figure 2.** Deformation mode (a) asymmetrical; (b) symmetrical

$F_m^d$  – average crushing force for;  $t$  – side-wall thickness;  $C, P$  – constant Cowper–Symonds relation.

In the crush analysis, a crucial issue is the deformation mode. The half-wavelength is associated with the geometric dimensions of the column presented by formula 9 [32]:

$$\frac{H}{t} = 0.99 \left( \frac{c}{t} \right)^{\frac{2}{3}} \quad (9)$$

## MATERIALS AND METHODS

Numerical analyses were led using Abaqus CAE. Each simulation was done in two steps, initially the buckling mode characteristic for the respective geometry was obtained, then the model with implemented geometric disturbance was subjected to dynamic crushing. The profile was between two rigid sheets working as top and base. It consisted in loading a non-deformable plate of mass 70 kg with an initial velocity of 7 m/s, resulting in mechanical energy of 1700 J. All profiles tested were loaded with the same energy and the analysis continued until the top lost velocity. The aim of the study was to determine the effect of the triggering position in the form of embossing on the behavior of the absorbers and the obtained crush efficiency indices. All analyses carried out were based on an explicit solver, whose operating principle is based on kinematic equations of motion. The results obtained are faster and more accurate than those of the implicit solver.

The models had a mesh size of 2.5 due to the accuracy of the results. Finite element of smaller

size significantly increased the duration of the analysis, as shown in Figure 4. The results presented are on the basis of sensitivity analysis carried out for a model with an initiator located 40 mm from the edge. There was a Tie relationship between the elements. Figure 3b shows a technical drawing of an aluminum thin-walled absorber with a trigger in the form of a spherical embossing. The shape of the initiator was fixed i.e. 32 mm in diameter and 3.6 mm deep (Figure 3a). The spherical embossment was inspired by a forming plastic joint. The crush stages visible during time-lapse analysis show that the generation of a folds involves the collapse of two opposite walls. The depth of an extrusion was a multiple of the column thickness (1.2 mm). Scientific studies show that the deeper the embossing, an improved crush initiator effect [11], hence an embossing depth of 3.6 mm was used. A greater depth was not possible due to the extrudability of aluminum. The variable parameter was the position of the center of the trigger relative to the base denoted by the parameter  $X$ , cases for the range 20–100 mm were studied. The initial size was due to geometrical constraints as the trigger had to fit all the way through, the maximum initiator position of 100mm was due to the fact that the authors wanted the column to start the initiation of the crushing process at its bottom.

The above table shows the numerical data on which the numerical model relies on. In the elastic field it is based on Young’s modulus and Poisson’s ratio (Table 1a), while in the strain range based on bilinear stress-strain relation (Table 1b). The results were obtained on the basis of self-tests realized on a tensile testing machine. The research was carried out according to PN-EN ISO 6892-1. Based on the

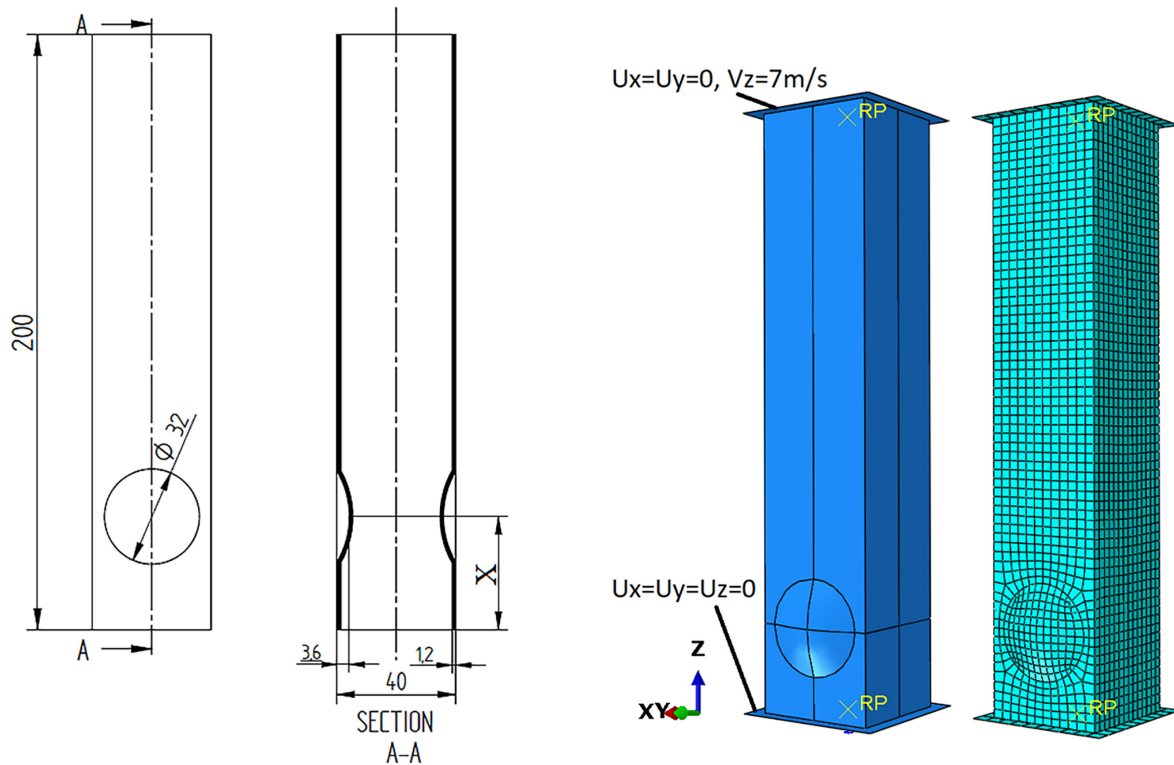


**Figure 3.** (a) Description of column geometry with embossing initiator; (b) the numerical simulation boundary conditions

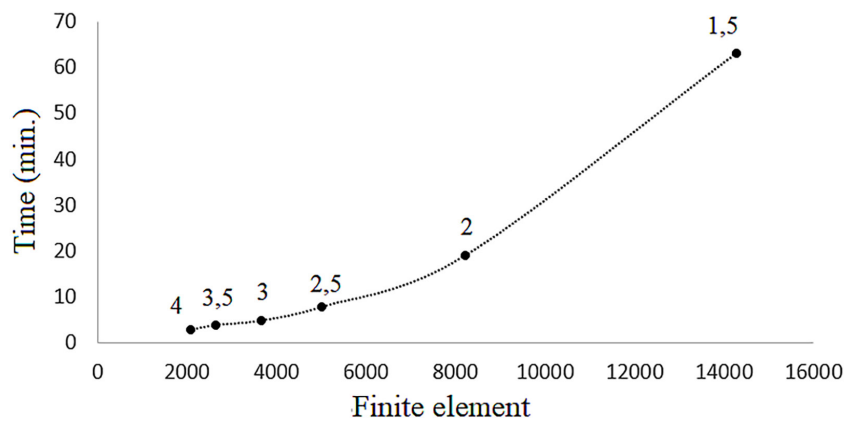


**Figure 4.** Sensitive analysis of finite element method

results of the tests of three specimens, the averaged values of bilinear stress-strain characteristics were determined (Table 1b). The manufacturing of thin-walled energy absorbers consisted of preparing profiles of a certain length, i.e. 200 mm, by cutting an extruded profile supplied by Sapa Company of Chrzanow, Poland. Next, using an aluminum matrix with a milled spherical surface, an embossing initiating the crush is made. The inserted die is positioned at the location determined for the occurrence of the trigger, then using a hydraulic press, the side walls are embossed to fill the die cavities

(Figure 5). The operation is repeated symmetrically on the other side and then the instrument is unscrewed and slid out of the two sides of the thin-walled profile. Based on numerical analyses, it was shown that the most advantageous position of the crush initiator defined by the x parameter in Figure 3a is 40 mm. For verification purposes, the model with such an initiator position was adopted for experimental testing.

The crush analysis was carried out using a Instron CEAST 9350HES stand, an overview is presented in graphic below (Figure 6). Load machine



Figure 5. Manufacturing process of embossed trigger

includes a tensometer detector connected to the chassis, which acquires necessary survey data. Additionally, the test stand had a striker where an additional mass is applied.

## NUMERICAL RESULTS

Based on the numerical analyses, indicators presented in more detail in section one were determined. The primary amounts rely on the running of the load curve. Figure 7 presents a compilation of characteristics for the trigger center position in the range 20-100 mm. Already on the basis of the graphs the variation in the formation of folds as a function of displacement is apparent. Moreover, it is possible to see the variation of the value of the total shortening of the profile for the exact amount of starting energy (1700 J).

The first indicator determined is PCF, that is the load discovered when crushing begins connected to geometry of column and position of the trigger. For the case studied, the force spread is in the range of 37.5 to 40.5 kN (Figure 8). A large force peak generated over a long period of time

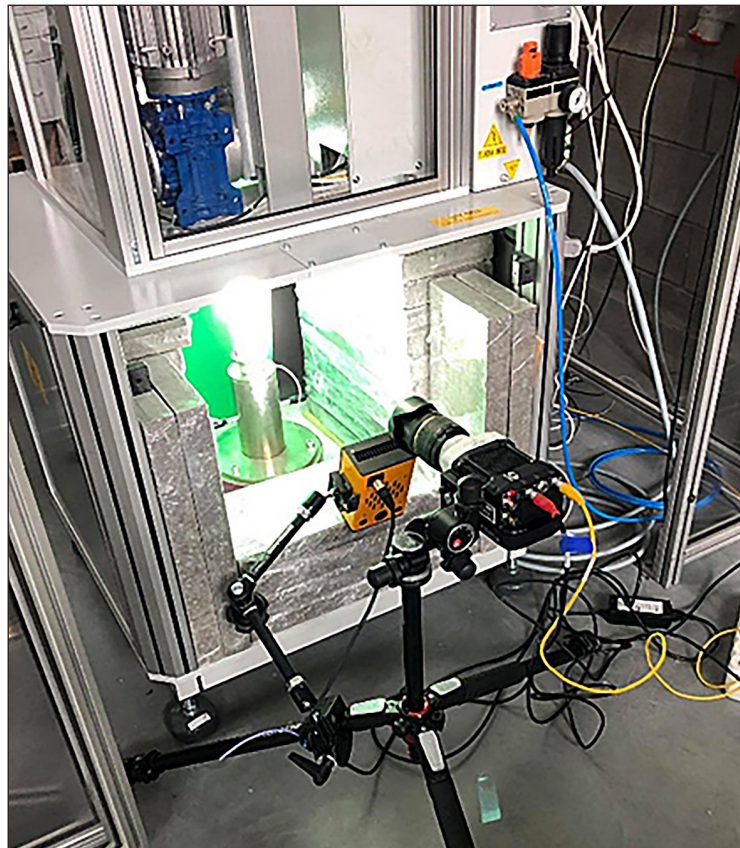
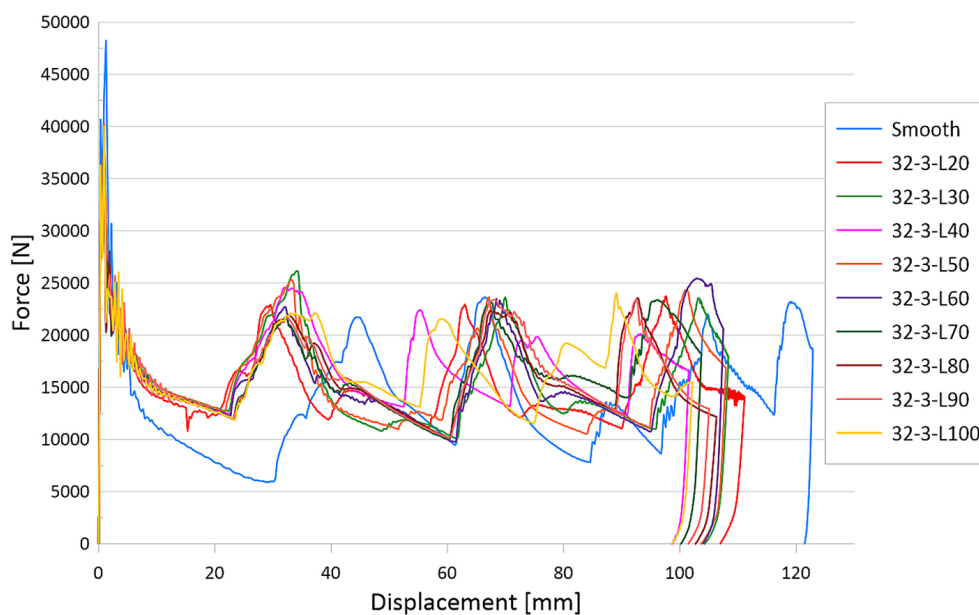


Figure 6. Dynamic testing machine with high-speed camera

**Table 1.** (a) Properties of aluminum profiles (own research); (b) plastic characteristics of profile material (self-study)

(a)	
AA. – 6063	
Density $\rho$ (kg/m <sup>3</sup> )	2700
Young's Modulus E (MPa)	70000
Poisson's Ratio (-)	0.33
(b)	
Stress $\sigma$ (MPa)	Strain $\epsilon$ (-)
200	0.00
249.40	0.0025
280.00	0.056

can cause fatalities. The graph shows that the thin-walled profile reaches the lowest value for the trigger position 40mm from the down edge. Figure 9 shows the mean crushing force, which reached values in the range of 15.25 to 16.75 kN. The value of the average force in the large miter is responsible for the overall performance of column. The higher its value, the higher the average force achieved during dynamic crushing. Due to the crush characteristics, thin-walled structures often show a large decrease in force after fold formation which is equivalent to a decrease in MCF. By using the shape of the trigger and its position it is possible to change its value significantly. The last indicator



**Figure 7.** Comparison of force curve for different trigger location

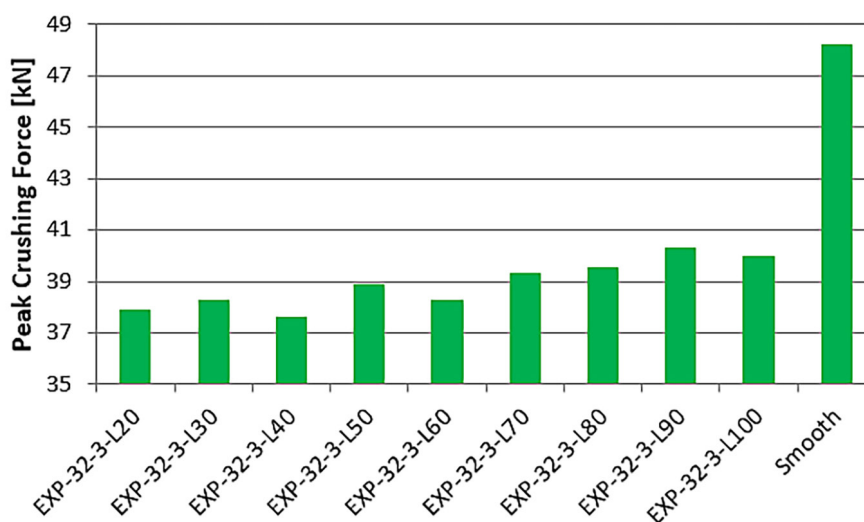


**Figure 8.** PCF value for different trigger location

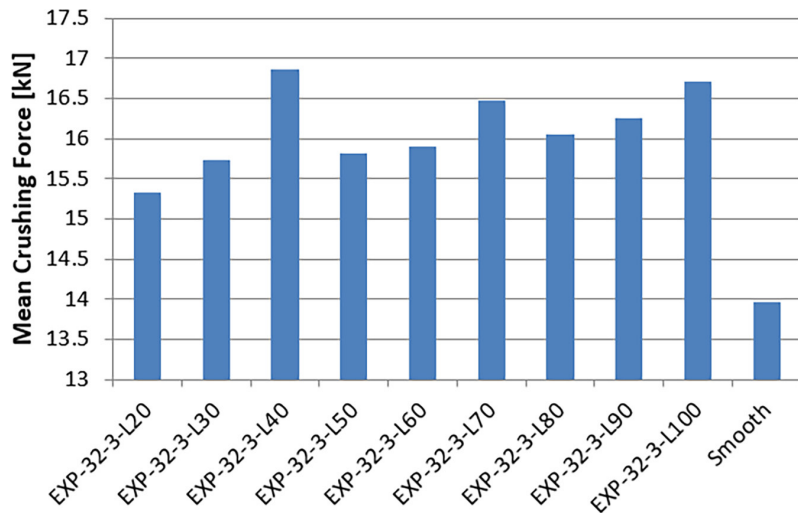


Figure 9. MCF value for different trigger location

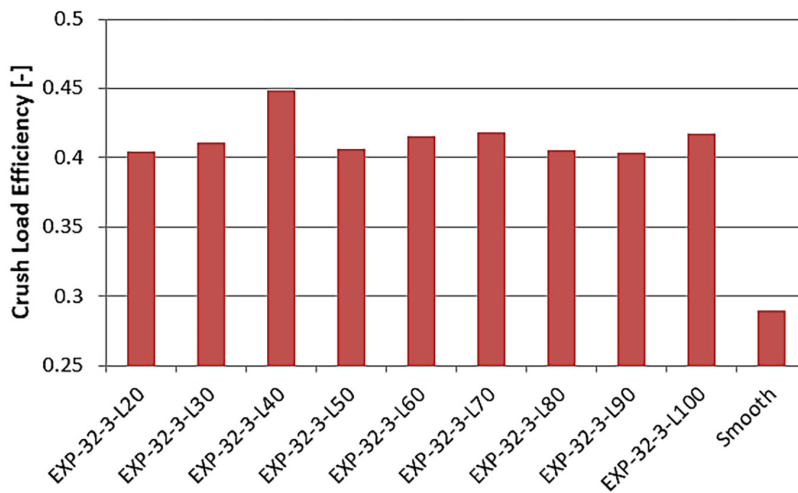


Figure 10. CLE value for different trigger location

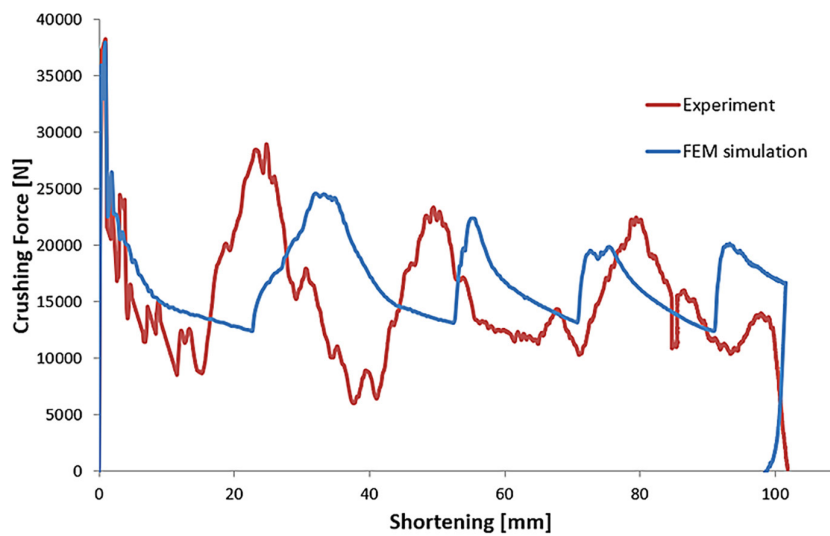


Figure 11. Numerical vs. experimental characteristics



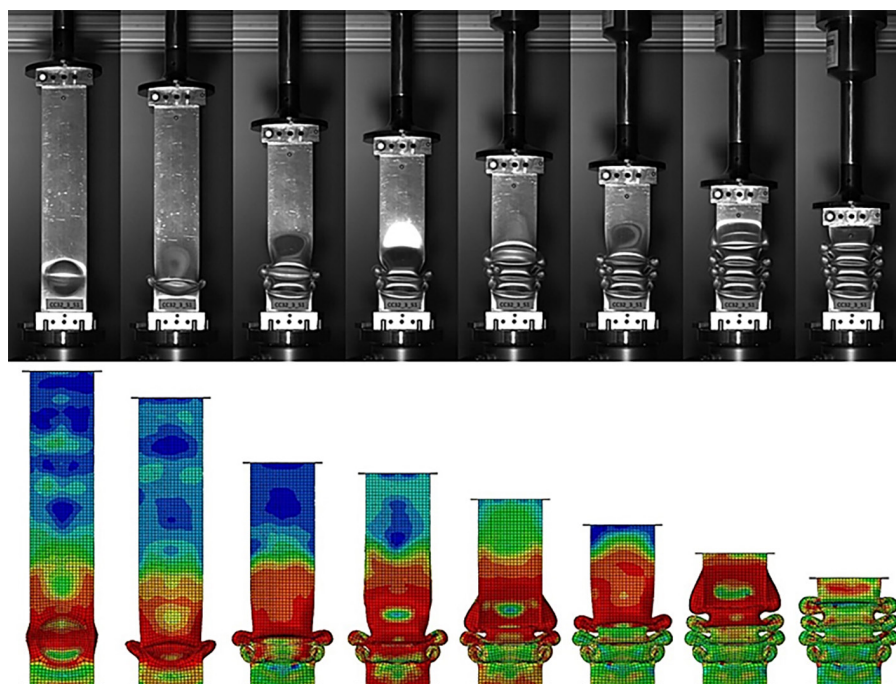


Figure 12. Crushing stages from experimental and numerical test

Table 2. Comparison of crashworthiness indicator of passive absorber

	EA [J]	PCF [kN]	MCF [kN]	CLE [-]	SE [-]
EXP	1689.9	38.281	16.602	0.434	0.509
FEM	1711.8	37.622	16.861	0.448	0.508
Difference [%]	1.29	1.72	1.56	3.34	0.27

determined is CLE which represents the crushing force efficiency (Figure 10). It significantly represents the thin-walled profile with the best force performance. The best effect is shown by the profile with the position of the trigger center at a distance of 40 mm from the down edge of the profile.

## EXPERIMENTAL RESULTS

Verification of the tested numerical models was carried out using the EXP-32-3-L40 model as an example (Figure 11), where the geometric dimensions of the embossing are 32 mm in diameter, 3.6 mm in depth, the position of the geometrical mean of the trigger is 40 mm from the base. The course of force relative to displacement values shown in Figure 11 confirms the correctly assumed conditions during the numerical analyses. The positive verification is evidenced by generation of fold as well as the characters accompanying the crush in the various stages of the collapse visible in Figure 12. On the waveform of

experimental force values, greater discrepancies are visible due to the sampling frequency of the sensor as well as the limitation of modeling the material in a simplified way to achieve a relatively low computational cost in numerical analysis. On the basis of the course of the two characteristics, the basic quantities described in the first section were determined, which unambiguously determine the energy-absorbing performance of the structure with a spherical embossed initiator. In addition to the values, the percentage difference was presented, which did not exceed 3.5% for the individual quantities. Particularly important magnitudes are the PCF value, which shows convergence at a high level, as well as the shape of the initial force peak seen in Figure 11 is very similar for both analyses. Another value indicating correct verification is the MCF index. The largest difference for the presented energy-absorbing indices is shown for the CLE, which results from the quotient of the average and maximum force values, so that the errors generated in the individual components are multiplied in the CLE index.

## CONCLUSIONS

The conducted numerical tests show that the best location of the trigger is a height of 40 mm from the absorber base. Determining the optimal height is related to the diameter of the press forming and the generation of an first fold. CLE value was identified as the most important optimization criterion. Figure 9 shows that the Crush Load Coefficient for a height of 40 mm increases the value of the CLE by about 15%, compared to a smooth column up to 50%. Optimal value of the trigger execution height assumed it also positively influences the values of PCF and MCF coefficients.

It should be also considered that the trigger height is related to the formation of the first fold. The numerical tests were verified on a dynamic test stand with a special time-lapse camera. In the experimental tests, the sample which revealed the greatest gains in crushing efficiency indicators was analyzed, i.e. with the trigger position 40 mm from the base. The study showed convergence at a very high level confirmed by the course of force versus displacement, comparative analysis of the various stages of the crush, as well as a tabulation of indicators characteristic of this type of analysis. The value discrepancy did not exceed 3.5% for both analysis. The presented research data reveal proper crush forcing can increase the performance of a thin-walled structure with

## Notation

$U$	– shortening of column,
$L_0$	– Initial length of a column,
$\sigma_d$	– dynamic yield stress,
$\sigma_s$	– static yield stress,
$\dot{\epsilon}$	– strain rate,
$C, P$	– constant Cowper-Symonds relation,
$2H$	– height of plastic hinge,
$t$	– sidewall thickness,
$c$	– two widths of the profile,
$\delta_c$	– crushing distance,
$I_1, I_3$	– integrals in equation 5,
$F_m^d$	– average crushing force for dynamic analysis,
$v_m$	– average velocity of tup,
$PCF$	– peak crushing force,
$MCF$	– mean crushing force,
$CLE$	– crush load efficiency,
$ANN$	– artificial neural network.

certain geometric parameters such as height and cross-section. This is especially important when the crush zone is limited, which is usually seen in automotive vehicles. Moreover, the presented results put the door open for further improvement of the structure, e.g. by filling the crash-box with porous in-situ/ex-situ materials. Energy absorbers designed in this way can serve in special vehicles, in rally vehicles, as well as in the space industry, where safety standards are high and the proposed solution is able to meet them.

## REFERENCES

- Alexander J.M. An approximate analysis of the collapse of thin cylindrical shells under axial loading. *Q. J. Mech. Appl. Math.* 1960; 13: 10–5.
- Wierzbicki T., Abramowicz W. On the Crushing Mechanics of Thin-Walled Structures. *J. Appl. Mech.* 1983; 50: 727–34.
- Abramowicz W., Jones N. Dynamic axial crushing of square tubes. *Int. J. Impact Eng.* 1984; 2: 263–81.
- Jones N., dos Reis H.L.M. On the dynamic buckling of a simple elastic-plastic model. *Int. J. Solids Struct.* 1980; 16: 969–89.
- Jones N. *Structural Impact* [Internet]. Cambridge, UK: Cambridge University Press; 1990.
- Macaulay M. *Introduction to Impact Engineering* [Internet]. Dordrecht: Springer Netherlands; 1987.
- Rogala M., Gajewski J., Górecki M. Study on the Effect of Geometrical Parameters of a Hexagonal Trigger on Energy Absorber Performance Using ANN. *Materials (Basel)*. 2021; 14: 5981.
- Kim H.S. New extruded multi-cell aluminum profile for maximum crash energy absorption and weight efficiency. *Thin-Walled Struct.* 2002; 40: 311–27.
- Marshall N.S., Nurick G.N.. Effect of induced imperfections on the formation of the first lobe of symmetric progressive buckling of thin-walled square tubes. *Int. Conf. Struct. Under Shock Impact, SUSI* 1998; 32: 155–68.
- Kaczyński P., Gronostajski Z., Polak S. Progressive crushing as a new mechanism of energy absorption. The crushing study of magnesium alloy crash-boxes. *Int. J. Impact Eng.* 2019; 124: 1–8.
- Ferdynus M., Gajewski J. Identification of crashworthiness indicators of column energy absorbers with triggers in the form of cylindrical embossing on the lateral edges using artificial neural networks. *Ekspluat. i Niezawodn.* 2022; 24: 805–21.
- Qureshi O.M., Bertocchi E. Crash performance of notch triggers and variable frequency progressive-triggers on patterned box beams during axial

- impacts. *Thin-Walled Struct.* 2013; 63: 98–105.
13. Rogala M., Gajewski J. Crashworthiness Analysis of Thin-Walled Square Columns with a Hole Trigger. *Materials (Basel)*. 2023; 16: 4196.
  14. Peixinho N., Soares D., Vilarinho C., Pereira P., Dimas D. Experimental study of impact energy absorption in aluminium square tubes with thermal triggers. *Mater. Res.* 2012; 15: 323–32.
  15. Nikkhah H., Baroutaji A., Kazancı Z., Arjunan A. Evaluation of crushing and energy absorption characteristics of bio-inspired nested structures. *Thin-Walled Struct.* 2020.
  16. Rogala M., Ferdynus M., Gawdzińska K., Kochmański P. The Influence of Different Length Aluminum Foam Filling on Mechanical Behavior of a Square Thin-Walled Column. *Materials (Basel)*. 2021; 14: 3630.
  17. Rogala M., Tuchowski W., Czarnecka-Komorowska D., Gawdzińska K. Analysis and Assessment of Aluminum and Aluminum-Ceramic Foams Structure. *Adv. Sci. Technol. Res. J.* 2022; 16: 287–97.
  18. Rogala M., Gajewski J. Numerical analysis of porous materials subjected to oblique crushing force Numerical analysis of porous materials subjected to oblique crushing force. *J. Phys. Conf. Ser.* 2021; 1736.
  19. Rogala M., Gajewski J., Gawdzińska K. Crashworthiness analysis of thin-walled aluminum columns filled with aluminum-silicon carbide composite foam. *Compos. Struct.* 2022; 299: 116102.
  20. Gajewski J., Golewski P., Sadowski T. The use of neural networks in the analysis of dual adhesive single lap joints subjected to uniaxial tensile test. *Materials (Basel)*. 2021; 14: 1–17.
  21. Rogala M., Gajewski J., Głuchowski D. Crushing analysis of energy absorbing materials using artificial neural networks. *J. Phys. Conf. Ser.* 2021; 1736: 012026.
  22. Gajewski J., Vališ D. Verification of the technical equipment degradation method using a hybrid reinforcement learning trees-artificial neural network system. *Tribol. Int.* 2021; 153.
  23. Yang M., Han B., Su P., Zhang Q., Zhang Q., Zhao Z., et al. Crashworthiness of hierarchical truncated conical shells with corrugated cores. *Int. J. Mech. Sci.* 2021; 193.
  24. Wysmulski P. Non-linear analysis of the postbuckling behaviour of eccentrically compressed composite channel-section columns. *Compos. Struct.* 2023; 305: 116446.
  25. Rozyło P. Failure phenomenon of compressed thin-walled composite columns with top-hat cross-section for three laminate lay-ups. *Compos. Struct.* 2023; 304: 116381.
  26. Wysmulski P. Numerical and Experimental Study of Crack Propagation in the Tensile Composite Plate with the Open Hole. *Adv. Sci. Technol. Res. J.* 2023; 17: 249–61.
  27. Falkowicz K. Experimental and numerical failure analysis of thin-walled composite plates using progressive failure analysis. *Compos. Struct.* 2023; 305: 116474.
  28. Wysmulski P. The analysis of buckling and post buckling in the compressed composite columns. *Arch. Mater. Sci. Eng.* 2017; 85: 35–41.
  29. Jonak J., Karpiński R., Wójcik A. Influence of the Undercut Anchor Head Angle on the Propagation of the Failure Zone of the Rock Medium—Part II. *Materials (Basel)*. 2021; 14: 3880.
  30. Jonak J., Karpiński R., Wójcik A. Influence of the Undercut Anchor Head Angle on the Propagation of the Failure Zone of the Rock Medium. *Materials (Basel)*. 2021; 14: 2371.
  31. Jonak J., Karpiński R., Wójcik A. Influence of Anchor Depth and Friction Coefficient Between Anchor and Rock on the Trajectory of Rock Masses Detachment. *Adv. Sci. Technol. Res. J.* 2023; 17: 290–8.
  32. Kopczyński A., Rusiński E. *Passive safety. Energy absorption by thin-walled profiles.* Wrocław: Publishing House of the Wrocław University of Technology; 2010.